Energetics and structure of organic molecules embedded in single-wall carbon nanotubes from first principles: The example of benzene

Matus Milko* and Claudia Ambrosch-Draxl

Chair of Atomistic Modelling and Design of Materials, Montanuniversität Leoben, Franz-Josef-Straße 18, A-8700 Leoben, Austria.

(Received 7 March 2011; revised manuscript received 27 June 2011; published 29 August 2011)

Stability and structural properties of nanopeapods are investigated by means of density-functional theory (DFT) including van der Waals interactions. As a prototypical system of organic π-conjugated molecules embedded into single-wall carbon nanotubes, we study benzene inside zig-zag nanotubes (n,0), with n ranging from 10 to 18. We explore the position and orientation of the molecule inside the cavity and find the optimal tube diameter for encapsulation to be around 1 nm. We compute that, overall, the molecule tends to align its molecular plane parallel to the tube axis. The internal orientation and molecule-wall distance depend, however, quite strongly on the tube diameter. The overall energy minimum is found for a situation in which the benzene ring takes a tilted position inside the (13,0) nanotube. Chirality turns out not to play a role in terms of the energetics. When benzene arrays are confined in nanotubes, the intermolecular distances can differ from those in the gas phase. Intermolecular interactions are important and further stabilize the peapods. As these as well as the molecule-tube interactions are governed by dispersive forces, we critically assess the performance of different DFT-based methods in this respect. Comparing four different computational schemes including both *ab initio* and semi-empirical treatment of van der Waals interactions, we conclude that vdW-DF is most reliable in terms of energetics and structural properties of these hybrids.

DOI: 10.1103/PhysRevB.84.085437 PACS number(s): 61.48.De, 71.15.Mb, 71.15.Nc

I. INTRODUCTION

Nanopeapods are hybrid systems consisting of a carbon nanotube (pod) with molecules or atoms (peas) accommodated in its cavity. Shortly after their first synthesis,[1] various attractive applications have been proposed. Combining the properties of their constituents makes nanopeapods suitable for optoelectronic devices.[2,3] After fullerenes and their derivates,[4] diverse peas have been embedded in nanotubes, ranging from ionic nanocrystals[5] and water/ice clusters[6] to organic molecules.[3,7]

In this work, we focus on the structural arrangements of such nanohybrids, as they are a crucial prerequisite for understanding their properties and function. Experimentally, the typical techniques for structural studies are transmission electron microscopy (TEM), Raman spectroscopy, and x-ray scattering, often complemented by calculations.[8,9] Among other computational approaches, density-functional theory (DFT) has been extensively used to investigate carbon nanotubes and peapods. Most of the work considering structural properties was focused on fullerene-based peapods.[10–13] A few exceptions to this are dedicated to organic oligomers and polymers,[3,14,15] linear hydrocarbon chains,[16,17] ionic nanocrystals,[18] and water particles[19,20] as possible peas.

Fullerenes, being nearly spherically symmetric, offer only restricted possibilities to detect and exploit new physics when forming nanohybrids. In contrast, anisotropic peas, like molecules, allow for exploring different structural configurations. Choosing representatives with interesting optical properties opens a perspective toward optoelectronic applications. In the latter case, π-conjugated molecules turned out to be excellent candidates.[3] Aiming at the understanding of peapod formation, we have chosen the benzene molecule, which is a simple example to explore bonding, geometry, and stability when embedded in a nanotube.

DFT is the most intensively used computational *ab initio* scheme in materials science. One of the major shortcomings of this approach was, until recently, the lack of an adequate description of van der Waals (vdW) interactions. (For simplicity, we use the term vdW synonymously for the long-ranged dispersive forces.) This interaction, however, is *the* binding mechanism in the systems under investigation.

Typically, common semilocal DFT functionals like the generalized gradient approximation (GGA) in various flavors fail badly for such weakly bound systems, while the local-density approximation (LDA) leads to binding with even reasonable interatomic distances. Therefore, LDA is frequently used for its remarkable results,[21] despite lacking full justification and discrepancies revealed for graphene-graphene interaction.[22] Hence, to date, only a handful of works are found in the literature that explicitly include corrections for the vdW forces when addressing structural issues of nanopeapods.

One option here is the application of a semi-empirical correction to the total energy. Such a scheme has, for example, been employed in calculations of encapsulated water chains and ice[20] as well as a model complex of methane[23] inside a nanotube. From the *ab initio* side, the so-called linear combination of atomic orbitals S^2+vdW method[24] was applied for a C_{60}-functionalized (10,10) nanotube,[25] as well as the vdW density functional[26] (vdW-DF) for the study of peapods with oligothiophenes encapsulated[3] and double-wall carbon nanotubes.[27]

In the following, we investigate the energetics of benzene-based peapods to gain insight into the structural arrangement of encapsulated molecules and molecular arrays, and to determine suitable tube sizes. To this extent, we employ vdW-DF[26] in comparison with common (semi)local DFT functionals as well as semi-empirical total-energy corrections.[28,29]

II. COMPUTATIONAL DETAILS

All self-consistent calculations presented here are performed within the framework of DFT, using Vanderbilt's ultrasoft pseudopotentials[30] as implemented in the program package QUANTUM ESPRESSO.[31] Valence electrons are expanded into a plane wave basis with a kinetic-energy cutoff of 30 Ry. Exchange-correlation effects are treated within LDA in the Perdew-Zunger parametrization[32] and GGA in the Perdew-Burke-Ernzerhof (PBE) flavor.[33]

To account for vdW interactions, we adopt two different approaches, both as post-processing after reaching the self consistency using PBE densities: In the vdW-DF proposed by Dion *et al.*[26] the nonlocal energy contribution is obtained from the mere knowledge of the electron density. We make use of an efficient implementation by Nabok *et al.*[34,35] based on Monte Carlo integration. Alternatively, we adopt a semi-empirical potential in two different parametrizations as suggested by Grimme[28,29] with the typical R^{-6} form, where a damping function ensures the correct asymptotic behavior for small interatomic distances R. We denote this method as DFT-D and, if needed, refer to the two different parametrizations as to DFT-D04 (Ref. 28) and DFT-D06 (Ref. 29).

We first relax the nanotubes and the benzene molecule separately with both LDA and GGA, respectively, such that all atomic forces become smaller than 1 mRy/Å. These geometries serve as starting points for structural relaxations of the corresponding peapods. We employ the supercell approach with the closest distance of two adjacent nanotubes being 8 Å. We consider a series of zig-zag nanotubes and denote the corresponding peapods as benz@(n,0) throughout. To achieve commensurability between nanotubes and molecular arrays, several settings of cell parameters have been chosen, varying from twice the elementary cell parameter $a_e = 4.26$ Å to several multiples. For the Brillouin zone integrations, we used 4, 3, or 2 k points for unit cell lengths of 2, 3, and 4 a_e, respectively.

The central quantity of our interest is the binding energy per unit cell

$$E_b = E_{\text{peapod}} - (E_{\text{tube}} + E_{\text{molecule}}), \qquad (1)$$

obtained by subtracting from the total energy of the peapod, E_{peapod}, the energies of its constituents, E_{tube} and E_{molecule}. With this definition, positive (negative) binding energy means that the peapod is unstable (stable).

III. RESULTS

A. Optimal tube size

Exploring the energetics and structural properties of molecules residing inside a nanotube, the first issue to be addressed is the range of tube diameters in which the resulting nanopeapod with a particular molecule of interest is stable. Such studies can guide experimentalists as they provide reliable estimates not only about reasonable nanotube sizes, but also about the affinity of the molecule to the internal space of its host.

The reliability of the results, however, can strongly depend on the computational scheme employed, especially on the treatment of vdW interactions. Thus, in this section, we compare the performance of four different DFT-based methods concerning their description of the dispersive forces. In the upper panel of Fig. 1, we present the binding energy for a series of peapods, labeled benz@(n,0), where n ranges from 10 to 18. The benzene molecule is placed in the middle of the tube, and the atomic positions are relaxed using LDA and PBE, respectively. For both, the relaxation effects are marginal for this molecular position. The only exception to this is benz@(10,0), where the molecule is found tilted by 90° resulting in a *lying* position, thereby heavily distorting the nanotube. Such a scenario, however, is unlikely to happen in reality as benz@(10,0) is predicted to be unstable by all methods, with an energy cost of at least 5.64 eV. For this reason, the corresponding results are not displayed.

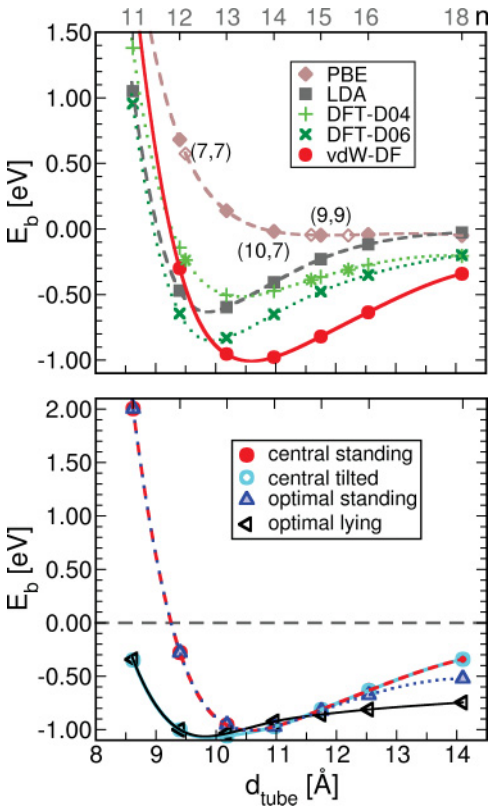

FIG. 1. (Color online) Top: Binding energy for a series of peapods, benz@(n,0), as a function of tube diameter resulting from PBE (brown diamonds), LDA (gray squares), DFT-D04 (light-green plus signs), DFT-D06 (dark-green crosses), and vdW-DF (red filled circles), respectively. In all cases, the molecule is located *standing* in the tube center. The open diamonds and the stars represent peapods with other chiralities, obtained by PBE and DFT-D04, respectively. The upper x axis indicates the index n of the chiral vector (n,0). Bottom: vdW-DF results for four different molecular arrangements as described in the text. For the *central standing* position the results are identical as in the panel above, the other curves represent the respective optimal orientation of the molecule and/or its distance to the tube wall.

GGA gives no binding, basically approaching the zero level asymptotically from above. LDA binds peapods of moderate size quite well, however, fails for larger tubes, which is in accordance with the findings of Girifalco and Hodak.[22] The obtained results are not surprising, recalling that LDA, despite

being a fully local functional, includes nonlocal correlations through a precise description of the exchange-correlation hole. Hence, for overlapping densities it works reasonably well, while it breaks down in the low-density limit. Here, the performance of LDA is as bad as PBE. Generally, LDA is comparable with DFT-D, except that the latter corrects for the wrong asymptotics. The two different versions of this scheme give qualitatively the same description although DFT-D06 (dark-green crosses) leads to stronger binding than DFT-D04 (light-green plus signs) in all our calculations. By far the largest binging energy is obtained by vdW-DF. The only exception to this is the short-distance region where it behaves more repulsively than LDA and DFT-D. Such finding has also been reported for molecular crystals.[34,36]

In addition to the zig-zag nanotubes, we have investigated peapods based on (7,7), (9,9), and (10,7) tubes. The results, indicated in Fig. 1 by the open diamonds (PBE) and stars (DFT-D), reveal that the chirality does not influence the structural properties of nanopeapods as they follow the same trends as the $(n,0)$ series. This finding is consistent with other results reported in the literature.[10,11]

The structural arrangement with the molecule residing in the middle of the tube may appear somewhat unrealistic, especially for larger tube diameters. Hence, in a next step, we compute the gain in binding energy when optimizing the distance between the molecule and the tube wall. Fixing the geometry of both subunits as resulting from the previous geometry relaxation, the energies are calculated for distances in steps of 0.01 Å. We investigate two different molecular orientations, the *standing* and the *lying* one (see Fig. 2). The molecule-wall distance d is defined as the xy-projected distance between the topmost atom of the nanotube and the topmost hydrogen of the benzene (standing position) or the molecular plane (lying position).

As depicted in Fig. 2, the interaction between the molecule and wall depends on the curvature, and hence the obtained distance varies with the tube diameter for both arrangements. For small nanotubes, [i.e., up to (12,0)] the most favorable position for both cases is found in the middle of the tube by both methods, LDA and vdW-DF. Starting from benz@(13,0) [benz@(14,0)], off-centered positions are favored by LDA for the lying (standing) molecule. vdW-DF finds the same trends, but the transition takes place for large tube sizes [benz@(14,0) and benz@(16,0), respectively], and this functional also leads to larger distances.

As no experimental data are available for peapods, a direct assessment of the functionals in terms of bond lengths and binding energies is not possible. Therefore, we evaluate their performance for systems closely related to the constituents. The most important examples here are graphite as well as organic molecules. In graphite, the interlayer spacing is very well reproduced by LDA, but the cohesive energy is largely underestimated, (i.e., more than a factor of 2 compared to Ref. 37). vdW-DF excellently reproduces the cohesive energy, while overestimating the separation between adjacent layers by nearly 7% (3.6 Å vs 3.36 Å, respectively).[38] LDA gives slightly too small lattice parameters for organic molecules in their solid-state packing (2.8% for pentacene and 4.6% for biphenyl). DFT-D behaves in a similar manner. vdW-DF shows the opposite trend.[34,36] The average deviation

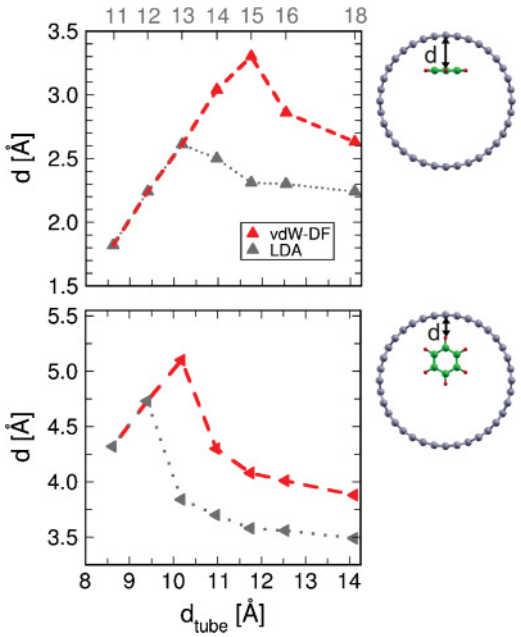

FIG. 2. (Color online) Top: Relation between optimal molecule-wall distance d and tube diameter d_{tube} for the lying (top) and standing (bottom) molecular position. The results depicted with red dashed line and gray dotted line correspond to vdW-DF and LDA, respectively. The definition of the respective distances is given to the right.

from experiment in the latter case is 2%, as obtained for molecular crystals formed by various oligomers of different lengths. The corresponding cohesive energies are very well reproduced by vdW-DF, as found for the oligoacene series,[34] but underestimated by LDA and DFT-D by at least 20%. The system most closely related to peapods, benzene on graphene, has been reported to be excellently described by vdW-DF.[39] In view of all these findings, we expect vdW-DF to be most reliable for the description of peapod formation, with the tendency of good energetics and only slightly too large bond lengths.

The bottom of Fig. 1 summarizes the overall stability of the peapods as obtained from vdW-DF. For each tube diameter, it depicts the most preferred configuration in terms of molecule-wall distance as well as spatial orientation. The role of the latter will be discussed in the following section. The most suitable diameter for the encapsulation of the benzene molecule is around 1.0 nm, corresponding to the (13,0) tube. Here, benzene tends to reside almost at the center, gaining most vdW energy from both nearly parallel sectors of the tube. As the superposition of the respective potentials gives rise to two minima for larger diameters, the molecule moves toward one of the walls. This also holds true for tilted and lying positions. The latter is very stable for small as well as large diameters, although the overall minimum is found for a particular tilted case.

Finally, we address the role of zero-point vibrations. To this extent, we consider the leading term, which is associated with the C-H bond stretching of the benzene ring. Starting from the relaxed structures of the molecule as well as the combined system, we stretch/compress the C-H bonds up to total displacements of 10^{-2} Å in steps of $2 \cdot 10^{-3}$ Å.

The corresponding 11 total-energy points are fitted to a second-order polynomial. Cross checking the second-order coefficient by higher-order fits, we could confirm that these displacements are within the harmonic regime in all cases considered here. The so-obtained corrections to the binding energy for all stable configurations are of the order of 0.01 eV. As an example, it amounts to 0.067, 0.026, 0.015 eV for (12,0), (13,0), and (16,0), respectively, in the standing configurations, (i.e., decreasing with increasing tube diameter as expected). Similarly, for the lying molecules, the respective contributions for (11,0) and (12,0) are 0.058 and 0.041 eV. Hence we can conclude that, overall, the zero-point energy does not significantly influence the stability of the investigated peapod systems.

B. Orientation of benzene inside the nanotube

In this section, we want to explore the preferred orientation of the molecule and its dependence on the nanotube size. To do so, we define two different angles, ϕ_x and ϕ_y, indicating the rotation of the molecule around the x and y axes, respectively. Because of symmetry, these two parameters need to run only between 0° and 90° to describe all possible molecular orientations at a fixed site. In the following, we will use the notation [ϕ_x, ϕ_y]. For this investigation, we use a unit-cell length of 2 nanotube repeat units, (i.e., 8.56 Å). Hence, adjacent molecules are separated by this distance in case of the standing position. The minimal separation corresponding to the case of [90°,0°] leads to a H-H distance of 3.53 Å. Our test calculations with larger unit cells have proved these distances to lead to negligible intermolecular interactions for any orientation (differences in binding energies below 1%).

In Fig. 3, the binding energy as a function of ϕ_x is plotted for four different peapods and the molecule in its central position. Here, each curve refers to a fixed ϕ_y value. Full symbols and lines represent vdW-DF-results. The smallest zig-zag nanotube capable of accommodating the benzene molecule is (11,0) with the lying orientation to be most stable, (i.e., gaining 2.5 eV in energy compared to the standing position). For the medium-sized peapods, the standing position is still most unfavorable. However, energy differences have become smaller, and the binding energies are negative throughout.

In benz@(12,0), a ϕ_y of 90° is preferred for all ϕ_x values, similar to the case of benz@(11,0), while the x axis tilts of 30° and 90° lead to a small energy gain. Inside the (13,0) tube, the energy differences become significantly smaller when the inclination exceeds 30° in either of the directions. As a representative of large peapods, benz@(15,0) is exemplified. Here the most preferable situation is achieved when the guest *stands*. Taking the lowest-energy point for each tube diameter yields the overall stability as depicted in the bottom panel of Fig. 1 (light blue spheres). The so-obtained curve exhibits the overall minimum associated with the (13,0) tube and tilting angles of [ϕ_x,ϕ_y] = [40,40].

To compare vdW-DF with the semi-empirical corrections, we show in Fig. 3 also the results for DFT-D in both versions, DFT-D04 depicted by the plus signs and dotted lines and DFT-D06 visualized by the crosses and dashed lines. For the sake of clarity, the complete set of results are displayed only for benz@(15,0). All other graphs contain the results for DFT-D

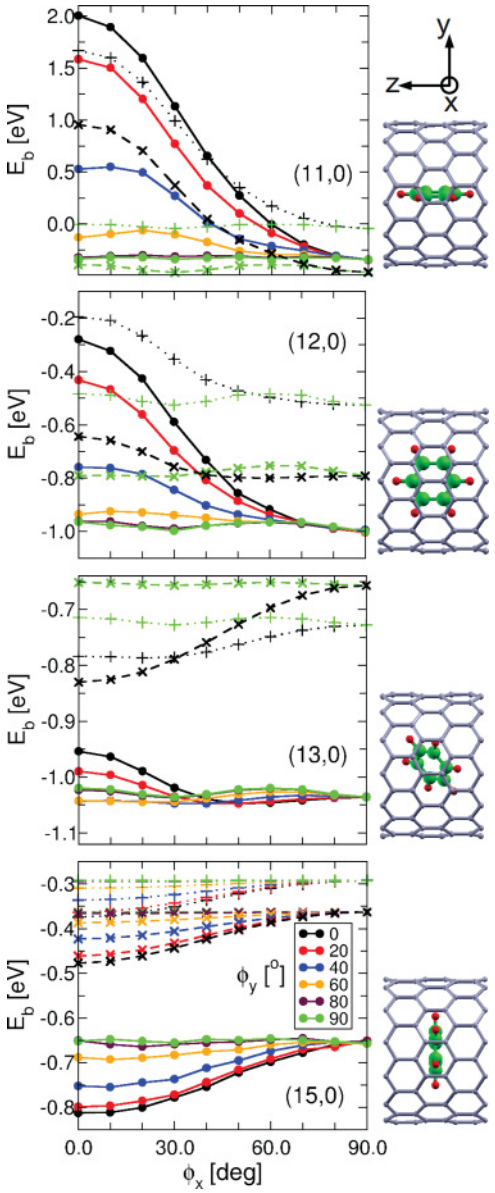

FIG. 3. (Color) Change in binding energy, E_b, when the benzene molecule is tilted around the x axis by the angle ϕ_x. The different full lines refer to vdW-DF results for different tilting angles ϕ_y around the y axis: 0° (black), 20° (red), 40° (blue), 60° (orange), 8°0 (violet), and 90° (green). The dashed and dotted lines indicate corresponding results from DFT-D06 and DFT-D04, respectively. Going from top to bottom, the four panels show the situation in benz@(11,0), benz@(12,0), benz@(13,0), and benz@(15,0). The schematics on the right side depict the preferred orientation for each case as determined from the respective overall energy minimum. The corresponding angles, [ϕ_x,ϕ_y], are [90, 0], [90, 90],[40], and [0, 0], respectively.

only for the limiting cases with $\phi_y = 0°$ and $\phi_y = 90°$. All other curves (not displayed) lie in between. In general, one can conclude that DFT-D in either parametrization gives the same trends as vdW-DF. In accordance with Sec. III A, it gives more binding for small peapods and less binding for medium and large-scaled systems. Again, the reason for this behavior rests

upon the fact that in the repulsive regime the vdW-D potential decreases more rapidly than vdW-DF (see top of Fig. 1).

Summarizing our findings from Fig. 3, the lying position is particularly favorable. In small peapods, it represents the, by far, most stable situation. Here, the dispersive forces are within the repulsive regime, and, hence, the lying ring minimizes energy by avoiding interaction of hydrogens with the tube wall. On the other hand, in larger peapods, the standing position is preferred over the lying one, but the energy differences are small. One should keep in mind, however, that considering the optimal molecule-wall distances, the lying orientation becomes significantly lower in energy (see Sec. III A). Such relaxation allows for the ideal long-range interplay of the highly polarizable π orbitals of the two subsystems.

Figure 3 also gives insight into the energy barriers for the rotation of the molecule inside the nanotube. It is obvious from the graphs that these barriers strongly depend on the tube diameter as well as on the rotational axis. The molecule may rotate freely around x in all peapods for $\phi_y = 90^\circ$, while the energy cost increases substantially for smaller ϕ_y, thereby strongly depending on tube size. As an example, the barrier of benz@(12,0) is 0.7 eV, while in (13,0) it is reduced to 0.1 eV. As one would expect, for small tubes it is quite difficult for the molecule to spin around freely. From the above values, one can estimate that the molecule inside the narrow (12,0) tube should stand still at temperatures below around 800 K, while inside (13,0) it can be expected to rotate already far below room temperature. Such behavior has indeed been observed by high-resolution TEM recently.[40] We should keep in mind that DFT calculations strictly refer to 0 K, and hence, our results do not account for entropy. While for the data discussed in Secs. III A and III C, it does not play a significant role, here the issue could become more important especially for large nanotubes where the rotational barriers are fairy small. On the other hand, for such large tubes one should consider two further facts which weaken the concern about entropic effects: First, with increasing tube diameter, the molecule tends to move toward the tube wall (see Sec. III A). Second, molecular arrays can form (see Sec. III C) which make rotations more improbable.

C. Arrangement of molecular arrays inside a nanotube

Our discussion up to now refers to a single molecule encapsulated in a nanotube. In this section, we want to explore embedded arrays of benzene rings in terms of their optimal intermolecular separation and spatial arrangement. Prior to further discussion, we have to disambiguate the definition of binding energy. The ambiguity results from considering more than one molecule, two in our case, in the unit cell. This gives two possible initial states leading to the formation of the peapod: (i) the whole molecular array in its optimal structure is inserted into an empty nanotube; (ii) two isolated benzene rings are inserted independently of each other. The corresponding binding energies, E_b, for the example of the standing benzene ring in a supercell with $a = 2a_e$ give values of -1.8558 and -2.0789 eV, respectively. For further investigations we only consider option (i).

We study the molecular arrays in three different arrangements, that is, with the benzene rings in the standing (A) and lying (B) positions, and inclined by 30° (C) as indicated in Fig. 4. As the host, we chose the (13,0) nanotube since it has proven to be most stable for accommodating benzene as discussed in the previous sections.

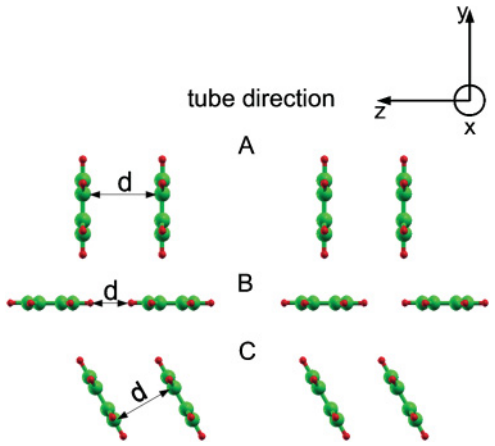

FIG. 4. (Color online) Schematic of three different benzene arrays, highlighting the definition of the corresponding intermolecular distances, d. A, B, and C refer to standing, lying, and 30°-inclined arrangements, respectively. For each case, two repeat units are shown.

The results are summarized in Table I. Here, we list the optimal intermolecular spacing of the arrays in both situations, that is, in gas phase ($d^{\rm opt}_{\rm array}$) and residing in the nanotube ($d^{\rm opt}_{\rm peapod}$), as well as their binding energies ($E^{\rm opt}_b$). $d^{\rm opt}_{\rm array}$ and $d^{\rm opt}_{\rm peapod}$ refer to the shortest intermolecular distances between the two closest hydrogen atoms as visualized in Fig. 3. Besides the three arrangements mentioned above, the corresponding values for the case benz@(13,0) with tilt angles of $\phi_x = \phi_y = 40^\circ$ are listed. The latter was found to be the most stable orientation for an isolated molecule inside the tube as discussed in the previous sections.

Comparing the intermolecular distances in the free-standing array with the embedded ones, the presence of the nanotube influences array B only negligibly, while in the other two cases the spacing increases more noticeably. The separation of the embedded molecules, $d^{\rm opt}_{\rm peapod}$, is larger by 0.06 and 0.15 Å for the arrangements A and C, respectively. As a matter of fact,

TABLE I. The optimal intermolecular distances for the free-standing molecular array, $d^{\rm opt}_{\rm array}$, and for an array inside the (13,0) nanotube, $d^{\rm opt}_{\rm peapod}$, the corresponding binding energy, $E^{\rm opt}_b$, the multiple of the elementary unit cell of this nanotube used in the calculation, $n_{\rm cell}$, and the resulting number of atoms in the supercell, $N_{\rm at}$, are listed for three different molecular arrays, A, B, C. For comparison, the results of a single molecule inside the tube are given as well. They correspond to the[40] arrangement, representing the overall optimal solution.

Arrangement	A	B	C	[40,40]
$d^{\rm opt}_{\rm array}$ [Å]	4.14	2.53	3.75	5.67
$d^{\rm opt}_{\rm peapod}$ [Å]	4.20	2.53	3.90	5.67
$E^{\rm opt}_b$ [eV]	−1.8779	−2.0899	−2.0144	−1.0473
$n_{\rm cell}$	3	4	3	2
$N_{\rm at}$	180	232	180	116

the formation of peapods turns out to be a subtle interplay between tube-wall as well as intermolecular interactions.

Before assessing the role of intermolecular interactions in the formation of peapods with encapsulated molecular arrays, we recall what we found so far for noninteracting molecules: Overall, the lying position was favorable, as it minimizes the repulsion between the molecule and the tube for small diameters, while it optimizes the attraction when the molecule moves toward the wall for larger tubes. Embedding molecular arrays can change this picture. Case B is comparable to the previous situation, as the intermolecular interaction is generally weak. In contrast, for the (13,0) case, investigated here, arrangement A becomes preferable due to enhanced intermolecular forces. This holds true even more for case C, where tilting of benzene leads to an additional energy gain of 136.5 meV. To judge upon the stability of the arrays, however, is not always straightforward. The problem is that, computationally, the structures A, B, and C require different supercells. Nevertheless, directly comparable are the binding energies of A with C, which are computed with the same unit cells as well as case B with the[40] peapod of noninteracting molecules, as their unit cells are commensurate. The latter is lower in energy by 4.7 meV. (Note that this binding energy has to be doubled to be comparable to the former.) We emphasize, however, that the quantities described above are typical for nanotube sizes close the that of (13,0). In larger peapods, where off-centered positions are likely to occur, various stackings of molecules are possible. In fact, such a situation has been experimentally observed and theoretically substantiated for peapods with sexithiophenes encapsulated.[3] Hence, also for our prototypical system, we expect the lying position to be realized, with the molecules organized in the cofacial arrangement. To systematically explore the energetics of different stacking configurations as a function of tube diameter, represents a challenge due to the huge number of degrees of freedom, and thus would go beyond the scope of the present paper.

IV. CONCLUSION

To conclude, we have performed a comprehensive study on the energetics and structural arrangements of the peapod model system benz@(n,0), with n between 10 and 18.

Investigating the size, it turns out that nanotubes with diameters of around 10 Å are most convenient to accommodate benzene and similar molecules, without any constraint with respect to chirality.

Although the molecular orientations as well as the molecule-wall distance depend quite strongly on the tube size, the lying position is particularly favored in both, small as well as large peapods. This is rationalized as follows: With the benzene ring fixed at the center, large peapods would prefer the standing position, while the small ones would require the molecule to lie. Taking the optimal molecule-wall separations into account, however, the situations turns around (i.e., the lying position is preferable overall).

The overall energy minimum with respect to tube diameter and molecular orientation is found to be benz@(13,0) with a tilt of 40 degrees around the x as well as y axes. Energy barriers for rotations of the molecule inside the cavity are found to strongly depend on the tube size. While molecules are not expected to spin up to several hundred degrees inside small tubes, rotations inside wider ones become more probable well below room temperature.

If arrays of molecules are considered, additional intermolecular interactions stabilize the nanopeapods. This way, molecular orientations with cofacial orientations become more probable. In contrast, this interaction is small for an array with lying benzene rings, and hence, the binding energy depends only weakly on the intermolecular distances in this case.

Finally, we want to assess the performance of different exchange-correlation functionals regarding such hybrid systems. Recalling the above comparison with related materials like graphite and molecular crystals, we arrive at the following conclusion. As cohesive energies from LDA and DFT-D deviate from the experiment by 20% for molecular crystals and even more for graphite, we expect a similar error bar of these functionals in the peapod formation. LDA exhibits the wrong asymptotics for large distances, and DFT-D only partially corrects this shortcoming. This fact represents a severe bottleneck for describing such weakly bound systems, as the density regime here strongly deviates from homogeneous charge distributions arising from distinctly overlapping wave functions. GGA must be ruled out to study the energetics and structure of vdW bound hybrids, even though it gives reliable densities and can be used for structural optimization of the constituents. Despite slightly overestimating bond distances, vdW-DF gives the most precise binding energies. We conclude that this scheme provides the most consistent results among the methods evaluated here.

ACKNOWLEDGMENTS

This work was carried out within the Nanoscience ERA project NaPhoD (Nanohybrids for Photonic Devices), financially supported by the Austrian Science Fund, Project No. I107. We thank D. Nabok for providing his implementation of the vdW-DF and J. Sofo for suggestions related to the effect of zero-point vibrations.

*matus.milko@unileoben.ac.at

[1] B. W. Smith, M. Monthioux, and D. E. Luzzi, Nature (London) **396**, 323 (1998).

[2] T. Shimada, T. Okazaki, R. Taniguchi, T. Sugai, H. Shinohara, K. Suendga, Y. Ohno, S. Mizuno, S. Kishimoto, and T. Mizutani, Appl. Phys. Lett. **81**, 4067 (2002).

[3] M. A. Loi, J. Gao, F. Cordella, P. Blondeau, E. Menna, B. Bártová, C. Hébert, S. Lazar, G. Botton, M. Milko, and C. Ambrosch-Draxl, Adv. Mater. **22**, 1547 (2010).

[4] K. Hirahara, K. Suenaga, S. Bandow, H. Kato, T. Okazaki, H. Shinohara, and S. Iijima, Phys. Rev. Lett. **85**, 5384 (2000).

[5]J. Sloan, M. C. Novotny, S. R. Bailey, G. Brown, C. Xu, V. C. Williams, S. Friedrichs, E. Flahaut, R. L. Callender, A. P. E. York, K. Coleman, M. L. H. Green, R. E. Dunin-Borkowski, and J. L. Hutschison, Chem. Phys. Lett. **329**, 61 (2000).
[6]Y. Maniwa, H. Kataura, M. Abe, S. Suzuki, Y. Achiba, H. Kira, and K. Matsuda, J. Phys. Soc. Jpn. **71**, 2863 (2002).
[7]K. Yanagi, K. Iakoubovskii, S. Kazaoui, N. Minami, Y. Maniwa, Y. Miyata, and H. Kataura, Phys. Rev. B **74**, 155420 (2006).
[8]M. Chorro, A. Delhey, L. Noe, M. Monthioux, and P. Launois, Phys. Rev. B **75**, 035416 (2007).
[9]L. G. Moura, L. M. Malard, M. A. Carneiro, P. Venezuela, R. B. Capaz, D. Nishide, Y. Achiba, H. Shinohara, and M. A. Pimenta, Phys. Rev. B **80**, 161401 (2009).
[10]W. H. Moon, M. S. Son, J. H. Lee, and H. J. Hwang, Phys. Status Solidi B **241**, 1783 (2004).
[11]M. Yoon, S. Berber, and D. Tománek, Phys. Rev. B **71**, 155406 (2005).
[12]S. Okada, M. Otani, and A. Oshiyama, New J. Phys. **5**, 122 (2003).
[13]M. Otani, S. Okada, and A. Oshiyama, Phys. Rev. B **68**, 125424 (2003).
[14]G. C. McIntosh, D. Tománek, and Y. W. Park, Phys. Rev. B **67**, 125419 (2003).
[15]W. Orellana and S. O. Vasquez, Phys. Rev. B **74**, 125419 (2006).
[16]T. C. Dinadayalane, L. Gorb, T. Simeon, and H. Dodziuk, Int. J. Quantum Chem. **107**, 2204 (2007).
[17]Y. Wang, Y. Huang, B. Yang, and R. Liu, Carbon **46**, 276 (2008).
[18]S. P. Huang, W. D. Cheng, J. M. Hu, Z. Xie, and H. Zhang, J. Chem. Phys. **129**, 174108 (2008).
[19]T. Kurita, S. Okada, and A. Oshiyama, Phys. Rev. B **75**, 205424 (2007).
[20]B. K. Agrawal, V. Singh, A. Pathak, and R. Srivastava, Phys. Rev. B **75**, 195420 (2007).
[21]S. Okada, S. Saito, and A. Oshiyama, Phys. Rev. Lett. **86**, 3835 (2001).
[22]L. A. Girifalco and M. Hodak, Phys. Rev. B **65**, 125404 (2002).
[23]S. Grimme, J. Antony, T. Schwabe, and C. Mück-Lichtenfeld, Org. Biomol. Chem. **5**, 741 (2007).
[24]Y. J. Dappe, M. A. Basanta, F. Flores, and J. Ortega, Phys. Rev. B **74**, 205434 (2006).
[25]Y. J. Dappe, J. Ortega, and F. Flores, Phys. Rev. B **79**, 165409 (2009).
[26]M. Dion, H. Rydberg, E. Schröder, D. C. Langreth, and B. I. Lundqvist, Phys. Rev. Lett. **92**, 246401 (2004).
[27]G. Roman-Perez and J. M. Soler, Phys. Rev. Lett. **103**, 096102 (2009).
[28]S. Grimme, J. Comput. Chem. **25**, 1463 (2004).
[29]S. Grimme, J. Comput. Chem. **27**, 1787 (2006).
[30]D. Vanderbilt, Phys. Rev. B **41**, 7892 (1990).
[31]P. Giannozzi, S. Baroni, N. Bonini, M. Calandra, R. Car, C. Cavazzoni, D. Ceresoli, G. L. Chiarotti, M. Cococcioni, I. Dabo, A. Dal Corso, S. de Gironcoli, S. Fabris, G. Fratesi, R. Gebauer, U. Gerstmann, C. Gougoussis, A. Kokalj, M. Lazzeri, L. Martin-Samos, N. Marzari, F. Mauri, R. Mazzarello, P. Paolini, A. Pasquarello, L. Paulatto, C. Sbraccia, S. Scandolo, G. Sclauzero, A. P. Seitsonen, A. Smogunov, P. Umari, and R. M. Wentzcovitch, J. Phys. Condens. Matter **21**, 395502 (2009).
[32]J. P. Perdew and A. Zunger, Phys. Rev. B **23**, 5048 (1981).
[33]J. P. Perdew, K. Burke, and M. Ernzerhof, Phys. Rev. Lett. **77**, 3865 (1996).
[34]D. Nabok, P. Puschnig, and C. Ambrosch-Draxl, Phys. Rev. B **77**, 245316 (2008).
[35]D. Nabok, P. Puschnig, and C. Ambrosch-Draxl, Comp. Phys. Commun. **182**, 1657 (2011).
[36]C. Ambrosch-Draxl, D. Nabok, P. Puschnig, and C. Meisenbichler, New J. Phys. **11**, 125010 (2009).
[37]R. Zacharia, H. Ulbricht, and T. Hertel, Phys. Rev. B **69**, 155406 (2004).
[38]S. D. Chakarova-Käck, E. Schröder, B. I. Lundqvist, and D. C. Langreth, Phys. Rev. Lett. **96**, 146107 (2006).
[39]D. C. Langreth, B. I. Lundqvist, S. D. Chakarova-Käck, V. R. Cooper, M. Dion, P. Hyldgaard, A. Kelkkanen, J. Kleis, L. Kong, S. Li, P. G. Moses, E. Murray, A. Puzder, H. Rydberg, E. Schröder, and T. Thonhauser, J. Phys. Condens. Matter **21**, 084203 (2009).
[40]J. Gao, P. Blondeau, P. Salice, E. Menna, B. Bártová, C. Hébert, J. Leschner, U. Kaiser, M. Milko, C. Ambrosch-Draxl, and M. A. Loi, Small **7**, 1807 (2011).